TISSUE ENGINEERING: Part A
Volume 23, Numbers 13 and 14, 2017

DOI: 10.1089/ten.tea.2016.0487

termis
Tissue Engineering
& Regenerative Medicine
International Society

ORIGINAL ARTICLE

Creation of a Bioengineered Skin Flap Scaffold with a Perfusable Vascular Pedicle

Bernhard J. Jank, MD,[1,*] Jeremy Goverman, MD,[2,*] Jacques P. Guyette, PhD,[1,*] Jon M. Charest, MS,[1] Mark Randolph, MAS,[3,4] Glenn R. Gaudette, PhD,[5] Joshua R. Gershlak, MS,[5] Martin Purschke, PhD,[6] Emilia Javorsky, MD, MPH,[6] Rosalynn M. Nazarian, MD,[7] David A. Leonard, MD,[4] Curtis L. Cetrulo, MD,[3,4] William G. Austen, MD,[2,3] and Harald C. Ott, MD[1,8]

Full-thickness skin loss is a challenging problem due to limited reconstructive options, demanding 75 million surgical procedures annually in the United States. Autologous skin grafting is the gold standard treatment, but results in donor-site morbidity and poor aesthetics. Numerous skin substitutes are available on the market to date, however, none truly functions as full-thickness skin due to lack of a vascular network. The creation of an autologous full-thickness skin analogue with a vascular pedicle would result in a paradigm shift in the management of wounds and in reconstruction of full-thickness skin defects. To create a clinically relevant foundation, we generated an acellular skin flap scaffold (SFS) with a perfusable vascular pedicle of clinically relevant size by perfusion decellularization of porcine fasciocutaneous flaps. We then analyzed the yielded SFS for mechanical properties, biocompatibility, and regenerative potential *in vitro* and *in vivo*. Furthermore, we assessed the immunological response using an *in vivo* model. Finally, we recellularized the vascular compartment of an SFS and reconnected it to a recipient's blood supply to test for perfusability. Perfusion decellularization removed all cellular components with preservation of native extracellular matrix composition and architecture. Biaxial testing revealed preserved mechanical properties. Immunologic response and biocompatibility assessed via implantation and compared with native xenogenic skin and commercially available dermal substitutes revealed rapid neovascularization and complete tissue integration. Composition of infiltrating immune cells showed no evidence of allorejection and resembled the inflammatory phase of wound healing. Implantation into full-thickness skin defects demonstrated good tissue integration and skin regeneration without cicatrization. We have developed a protocol for the generation of an SFS of clinically relevant size, containing a vascular pedicle, which can be utilized for perfusion decellularization and, ultimately, anastomosis to the recipient vascular system after precellularization. The observed favorable immunological response and good tissue integration indicate the substantial regenerative potential of this platform.

Keywords: dermal matrix, acellular matrices, decellularized, skin scaffold

Introduction

In the United States, chronic wounds alone affect 6.5 million patients and close to 75 million surgical procedures are performed annually to treat acute wounds, burns, and soft tissue loss caused by trauma.[1] The gold standard for the treatment of full-thickness cutaneous wounds is autologous skin grafting. While split-thickness skin grafts (STSGs) allow for coverage of large wounds, they only transplant a small portion of the dermis and therefore are subject to significant scarring and contracture. Full-thickness skin grafts (FTSGs) transplant the epidermis and the entire

[1]Center for Regenerative Medicine, Massachusetts General Hospital, Harvard Medical School, Boston, Massachusetts.
Divisons of [2]Burns and [3]Plastic Surgery, Department of Surgery, Massachusetts General Hospital, Harvard Medical School, Boston, Massachusetts.
[4]Center for Transplantation Sciences at Massachusetts General Hospital, Boston, Massachusetts.
[5]Worcester Polytechnic Institute, Worcester, Massachusetts.
[6]Wellman Center for Photomedicine, Boston, Massachusetts.
[7]Department of Pathology, Massachusetts General Hospital, Harvard Medical School, Boston, Massachusetts.
[8]Division of Thoracic Surgery, Department of Surgery, Massachusetts General Hospital, Harvard Medical School, Boston, Massachusetts.
*These three authors contributed equally to this work.

dermis and are therefore subject to less contracture resulting in a more functional and cosmetic final outcome; however, FTSGs are dependent on vascular ingrowth and inosculation of donor and host vessels, and are limited by donor-site availability. Similarly, local and distant fasciocutaneous flaps can be used to cover full-thickness cutaneous defects but are also limited by donor-site availability and associated donor-site morbidity.[2]

A number of skin substitutes and dermal matrices have been produced and commercialized, yet none has truly functioned as full-thickness skin. Current acellular dermal matrices, or dermal equivalents, lack epithelium and require at least 3 weeks for host incorporation. During this period of time, the template undergoes degeneration and cicatrization, risking infection and resulting in replacement of dermal template with a layer of scar. This scar layer provides little structural support, does not prevent contracture of the underlying wound or overlying skin graft,[2–4] and still requires a STSG for complete wound closure. Attempts to prevascularize acellular dermal constructs have been described, however, with limited success. Most notably lacking is the ability to easily access the pre-existing microvascular network via a macrovascular connection.

Given the immense economic and social impact of wounds, burns, and scarring in our society, the creation of a bioengineered autologous full-thickness skin analogue remains of paramount importance, has the potential to eliminate the need for donor sites and reduce morbidity from scarring and contracture, and would result in a paradigm shift in the management of wounds and skin loss from multiple causes.

Perfusion decellularized matrices have previously been utilized for the regeneration of whole organs[5–10]; however, these platforms may also serve as scaffolds for the generation of FTSGs. Appropriate cells to regenerate fasciocutaneous tissue *in vitro*, such as endothelial cells,[11] mesenchymal cells,[12] and keratinocytes,[13] can already be isolated from patients. The ability to utilize autologous explanted microcirculatory beds as vascularized bioscaffolds in the form of microvascular free flaps has previously been demonstrated in three studies.[14–16] One of these studies utilized perfusion decellularization to generate an acellular scaffold from a fasciocutaneous free flap in a rat model. Biomechanical properties, biocompatibility, immunological response, and regenerative potential of such a construct are yet to be tested.

Given these promising results, we therefore aimed to generate such a scaffold of a clinically relevant size in a porcine model. Based on our experience with composite tissue engineering,[5] we developed a protocol for the generation of a full-thickness porcine skin flap scaffold (SFS) with a perfusable vascular pedicle. We isolated fasciocutaneous skin flaps with a dominant vascular pedicle from the groin of adult pigs. The flaps were then perfused with a sequence of detergents via the vascular pedicle. Perfusion decellularization led to the removal of cellular material, creating acellular full-thickness SFS with preserved biomechanical properties, matrix ultrastructure, and biochemistry. Furthermore, we demonstrate substantial regenerative potential, both *in vitro* and *in vivo*. In a final experiment, we attempt to re-endothelialize an SFS and anastomose it to a recipient's blood supply in orthotopic position (Fig. 1).

Materials and Methods

Study design

The overall study design is shown in Figure 1. We harvested fasciocutaneous flaps and performed perfusion decellularization via the vascular pedicle. Following protocols we established in whole-organ decellularization,[17] we first characterized scaffold composition and architecture. We then performed *in vitro* biocompatibility and mechanical testing of the resulting decellularized SFSs, and went on to evaluate their regenerative potential. Current commercially available matrix products served as control. As a next step, we aimed to assess the immunological response to the SFS and its regenerative properties after implantation in an immunocompetent rat model *in vivo*. In a final experiment, we re-endothelialized SFSs and attempted to transplant them into orthotopic position in recipient pigs.

Organ harvest and perfusion decellularization

Research animals were selected from the MGH miniature swine herd.[18] MGH miniature swine are bred in a specific pathogen-free facility with defined major histocompatibility complex (MHC) while maintaining minor antigen variation. Animals were housed at the Transplantation Biology Research Center in accordance with the Guide for the Care and Use of Laboratory Animals. All experiments were conducted in accordance with the guidelines set by the Committee on Laboratory Resources, US National Institutes of Health, and Subcommittee on Research Animal Care and Laboratory Animal Resources of Massachusetts General Hospital.

A fasciocutaneous vascularized composite groin flap model was harvested as previously described.[19] Briefly, donor animals were placed under general anesthesia, positioned supine with the hind limbs extended and prepared for surgery. A skin island of $\sim$10–18 cm was elevated, with the underlying subcutaneous tissue and fascia, on a vascular pedicle comprising the medial saphenous artery and veins to their junctions with the superficial femoral vessels. Before transection of the vascular pedicle, the animals were systemically heparinized. Flaps were recovered and flushed with 100 U/mL heparin sulfate in 0.9% normal saline before transportation to the laboratory for decellularization.

Perfusion decellularization was performed as per a previously described composite tissue protocol.[5] Flaps were cannulated with prefilled 20G cannula (Luer Stubs; Harvard Apparatus/Instech) using a surgical microscope and flushed with sterile phosphate-buffered saline (PBS) for 2 h to remove all remaining blood. Subsequently, perfusion with 1% sodium dodecyl sulfate (Sigma Aldrich) was started for 10 days at a constant flow of 1.5–3 mL/min. Then, flaps were flushed with 2 L of deionized water before 1 day of perfusion with 1% Triton X-100 (Sigma Aldrich). This was followed by another 2 L of deionized water and 6 L of PBS to wash out all remaining detergents. All washing steps were performed in a single-pass manner.

Scaffold analysis and characterization

For DNA quantification, tissue samples were taken from native and decellularized skin flaps and from the products Alloderm® (A) and Permacol® (P). Colorimetric assays were used to determine elastin (Fastin; Biocolor), sGAG

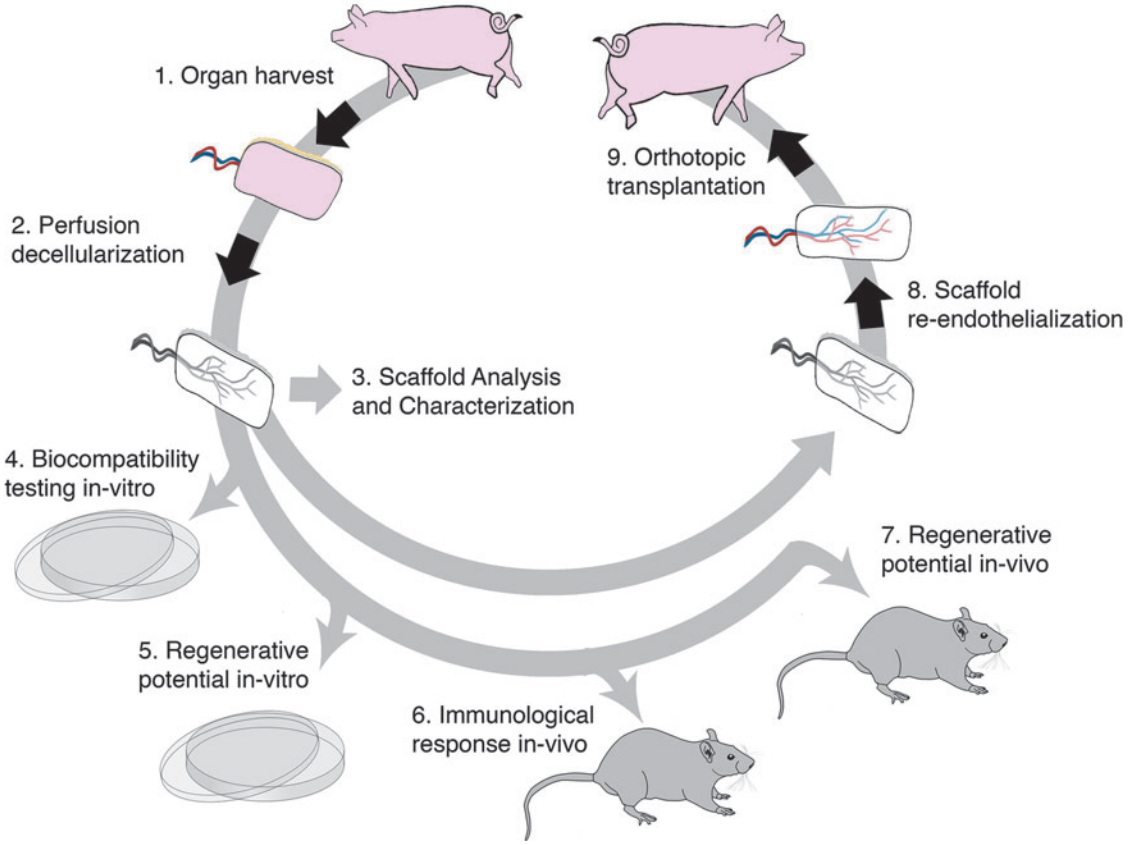

FIG. 1. Study overview. Full-thickness skin flaps were harvested with a vascular pedicle from the groin of donor pigs **(1)** and perfusion decellularized **(2)**. The resulting matrix was analyzed for biochemical composition, biomechanical properties, and histologic ultrastructure **(3)**. Samples were tested for biocompatibility *in vitro*, using hMSCs **(4)**. The acellular, papillary dermis was tested for its potential to allow for human keratinocyte integration and formation of a stratified layer, *in vitro* **(5)**. *In vivo* immunologic response of a xenogeneic recipient (rat) to our acellular matrix was tested **(6)**. *In vivo* regenerative potential of our acellular matrix was tested via implantation into full-thickness skin defects **(7)**. Finally, we attempt to re-endothelialize SFSs **(8)** and anastomose them to the blood supply of recipient animals to test for reperfusion **(9)**. hMSCs, human mesenchymal stem cells; SFS, skin flap scaffold.

(Blyscan assay; Biocolor), and insoluble collagen (Sircol assay; Biocolor) content.

Biaxial mechanical testing

Two-dimensional tensile testing was performed on native and decellularized skin grafts, as well as two commercially available dermal substitutes. Loads were applied biaxially (1:1 ratio of x-load to y-load) under stress control up to 20 kPa. Forces along the axes were measured with torque transducers, and movement of the graphite particles was measured using a CCD camera. Stress was calculated as the force acting on the cross-sectional area and strain was calculated as the change in length divided by the original length at the tare load. For each sample, moduli were calculated as the slope of the linear region of the stress–strain curve.

In vitro—*biocompatibility testing*

Decellularized FTSGs were embedded in Tissue-Tek® O.C.T. compound, cut into 100 μm sections to allow for optimal permeation of the resazurin reagent, and transferred into a six-well plate. Human mesenchymal stem cells (hMSCs) were then seeded directly onto each tissue slice or tissue culture plastic. Cells were allowed to attach for 60 min, after which we added 3 mL of medium to each well and cultured seeded tissue slices for up to 21 days under standard culture conditions. Resazurin reduction assay was performed every other day and fluorescence of medium was read using a SpectraMax Microplate Reader (Molecular Devices) at 544 nm (ex) and 590 nm (em).

Immunological response testing

Tissue samples from perfusion decellularized porcine flaps, native porcine skin, Permacol, and Alloderm were prepared and implanted into the subcutaneous tissue of Sprague Dawley (SD) rats. For the sham group, skin incisions were made followed by blunt dissection of the subcutaneous tissue but without implantation of any material. After 14 days, animals were sacrificed, blood samples were taken, and the implants were harvested with the surrounding native skin and subcutaneous tissue for histological analysis. For the sham group, the wound area with the adjacent subcutaneous tissue was harvested for analysis.

Epidermal permeability barrier

Biotin (Long Arm NHS; Vector Laboratories) was reconstituted to 50 μg/μL and applied to the epithelial side of the native, decellularized, and regenerated samples for

1 min. Tissue was washed 3×5 min in PBS, fixed in 10% formalin (Fisher Scientific) over night, and paraffin embedded. Six micrometer sections were cut on a microtome, deparaffinized, rehydrated, and stained with 594 Streptavidin (1:400; Life Technologies) for 40 min. Sections were then washed 3×10 min with PBS and mounted using aqueous mounting media containing DAPI (Fluoromount; Southern Biotec). Images were taken on a Nikon Ti-E inverted fluorescent microscope.

In vitro *reconstruction of epidermis*

Decellularized full-thickness skin samples were trimmed to a thickness of $\sim 1000\,\mu m$, such that only the papillary dermis remained. The resulting dermal grafts were transferred to six-well plates, seeded with keratinocytes, fully submerged and cultured for 7 days, and then exposure to the air/liquid interface and to induce formation of a stratified layer.

Full-thickness skin defect model

Under general anesthesia, circular 6 mm full-thickness skin was excised from the dorsal surface of SD rat and equal size biopsies from perfusion decellularized full-thickness skin grafts were sewn into the defects. Sterile wound dressing was removed after 4 days and sutures were removed after 14 days. Quantification of cellular infiltration into the implanted grafts, as well as histology, immunofluorescence, and immunohistochemistry were performed on excised tissue samples. Quantification of immune cell infiltration was also performed via staining for either CD68 (MCA341GA, 1:50; AbD Serotec) or CD3 (ab16669, 1:100) and imaged using immunofluorescence (Alexa-Fluor anti-rabbit 594 and anti-mouse 594). A custom CellProfiler (http://cellprofiler.org)[20] image analysis pipeline based on the work of Jones *et al.*[21] was developed to identify nuclei and cytoplasm objects within each image.

Re-endothelialization and experimental transplantation of SFS

SFSs were perfused with endothelial growth medium under standard culture conditions overnight before cell seeding. Cell seeding was performed as follows: 40 million human umbilical vein endothelial cells (HUVECs) were suspended in endothelial growth medium and infused into the vascular pedicle of SFS via gravity perfusion at 110 mmHg. HUVECs were used for this initial experiment because of our experience with this cell line in short-term transplantation experiments into porcine recipients. Static cell culture for 2 h allowed for cell attachment, which was then followed by perfused tissue culture for up to 5 days. At the day of transplantation, SFSs were flushed with ice-cold saline and transferred to the operating room. Recipient vessels were prepared in orthotopic location of MGH miniature swine and SFSs were connected to the recipient vessels using a direct cuff technique.

Statistical analysis

Student's *t*-test was performed using Microsoft Excel for Mac 2011. One-way analysis of variance and Bonferroni multiple comparison tests were performed using STATA 13 (StataCorp LP).

Results

Perfusion decellularization and matrix characterization

Fasciocutaneous flaps were harvested from the groin of adult pig, transferred into a custom-made decellularization chamber, and decellularized via the vascular pedicle using a previously described composite tissue protocol.[5] During the decellularization process, the tissue expanded due to the removal of cellular structures, gradually lost opacity, but remained morphologically intact (Fig. 2a). Histologic examination and scanning electron microscopy (SEM) revealed full preservation of dermal and subcutaneous ultrastructure while the epidermal layer was removed, leaving behind the intact papillary dermis (Fig. 2b–d). No nuclei were detectable on histologic examination (Fig. 2c, high-power fields). Verhoeff's elastic staining revealed the preservation of elastic fibers after decellularization (Fig. 2b, c, high-power field). Immunofluorescence microscopy for extracellular matrix (ECM) proteins confirmed the preservation of collagen I, collagen III, laminin, and elastin in comparable structural configuration as seen in native skin (Fig. 3a–d).

Preservation of ECM proteins plays an important role in maintaining the mechanical properties of an engineered scaffold and serves to encourage appropriate tissue integration.[22] Biomechanical properties of our decellularized SFSs (''Dec'') were measured via biaxial testing and compared to native porcine skin (''Nat'') and two commercially available acellular dermal substitutes: a crosslinked porcine-based dermal matrix (Permacol) and an acellular human dermal matrix (Alloderm). Young's modulus was used to determine the stiffness during material testing. The SFS was found to be similar to that of native porcine skin and Alloderm, whereas Permacol was found to be significantly more stiff (Fig. 2e).

Biochemical analysis showed a decrease of double-stranded DNA from 1877 ± 509 ng/mg dry tissue in native porcine skin to 455 ± 86 ng/mg dry tissue ($n = 3$, $p < 0.001$) in the SFS. In comparison, Permacol had a residual DNA content of 63 ng/mg dry tissue ($n = 1$), while Alloderm had a residual DNA content of 960 ng/mg dry tissue ($n = 1$) (Fig. 3e). For ECM proteins, our decellularization protocol retained 98% of insoluble collagen (404 ± 88 vs. $399 \pm 104\,\mu g$/mg wet weight, $n = 3$) (Fig. 3h). Sulfated glycosaminoglycans could be retained to 56% (4.87 ± 0.66 vs. $2.73 \pm 0.79\,\mu g$/mg wet weight, $n = 3$, $p = 0.03$) (Fig. 3g). Elastin decreased to 30% (3.14 ± 0.39 vs. $0.94 \pm 0.75\,\mu g$/mg wet weight, $n = 3$, $p = 0.01$) of native porcine skin (Fig. 3f).

SEM of native and decellularized full-thickness samples showed removal of the epidermis with complete structural preservation of the dermis (Fig. 2d, top row, right). In addition, intradermal ECM configuration was morphologically preserved after decellularization (Fig. 2d, bottom row).

Biocompatibility testing

As a first step toward bioengineering a skin flap, we aimed to test the scaffold's biocompatibility on tissue slices *in vitro*, using hMSCs and a resazurin-based viability assay. One hundred micrometer slices of SFS were attached to single wells of six-well plates and seeded with 4×10^5 hMSCs (Fig. 4b, d). As a control, we seeded the same cells on culture plastic and expanded them over the course of 21 days (Fig. 4a). No differences were noted in the calculated growth curve between the two groups ($n = 3$), suggesting full biocompatibility of the

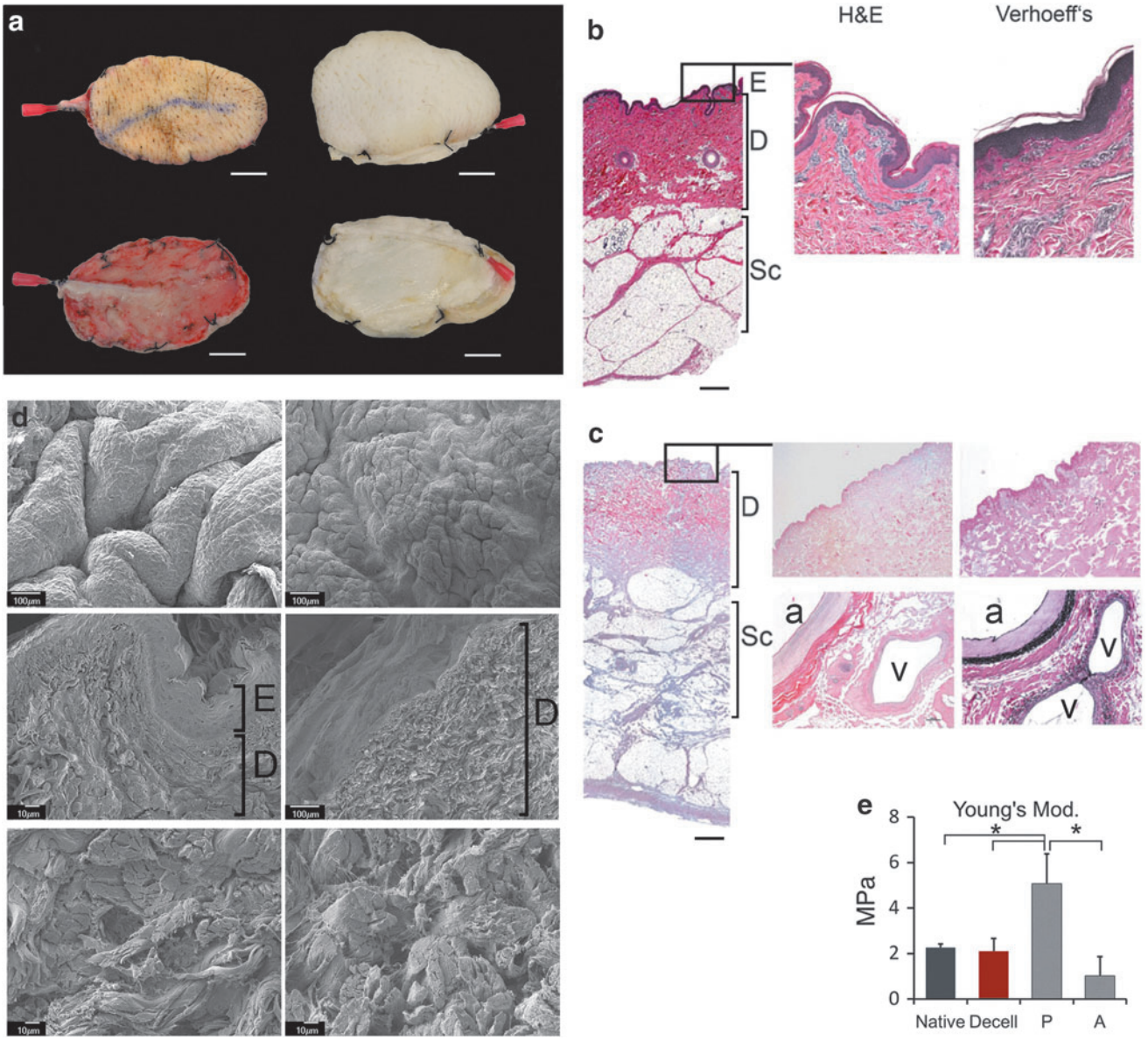

FIG. 2. Perfusion decellularization of full-thickness skin grafts. **(a)** Photographs of isolated skin grafts, cannulated for perfusion decellularization, *top* view = epidermal side, *bottom* view = subcutaneous side. Perfusion decellularization yielding white, acellular scaffolds after 10 days of detergent perfusion. H&E-stained full-thickness cross sections of native **(b)** and decellularized **(c)** skin flaps as overview (*left*) with high-power field (*right*). Verhoeff's elastic staining of the same sections in high-power field. *Black bars* mark epidermis (E), dermis (D), and subcutaneous tissue (Sc). Arterial (a) and venous (v) lumen are preserved. **(d)** Scanning electron microscopy of native (*left*) and decellularized (*right*) skin flaps in top-view (*top row*) dermo–epidermal cross section (*middle row*) and intradermal high-power field cross section (*bottom row*). **(e)** Biomechanical analysis of the elastic modulus for native and decellularized skin flaps and comparison with commercially available product Permacol® (P) and Alloderm® (A). ($n > 3$ for all samples, values are mean ± standard deviation, *asterisk* indicating $p < 0.05$). Scale bars 2 cm **(a)**; 1000 µm **(b, c)**. H&E, hematoxylin and eosin.

acellular scaffold (Fig. 4c). Staining of the cells with calcein after 8 days of culture revealed different morphology of cells growing in the scaffold compared to cells on plastic (Fig. 4a, b). Hematoxylin and eosin staining showed migration of the cells into the dermal ECM (Fig. 4d, black arrowheads).

Regenerative potential testing

The crucial function of skin is to provide barrier function against the environment (i.e., providing protection against dehydration, microorganisms, and toxins).[23] To support fluid homeostasis, prevent infection, and to integrate as a graft, tissue-engineered skin must restore barrier function as quickly as possible.[24] To examine the ability of the SFS to restore barrier function, we performed two experiments. First, we tested the SFS for its ability to allow human keratinocyte engraftment and formation of a multilayered, stratified epidermis-like structure *in vitro*. Second, we tested the SFS for its regenerative performance when implanted into a full-thickness skin defect *in vivo*. Barrier function was evaluated using a biotin permeability assay.[25,26]

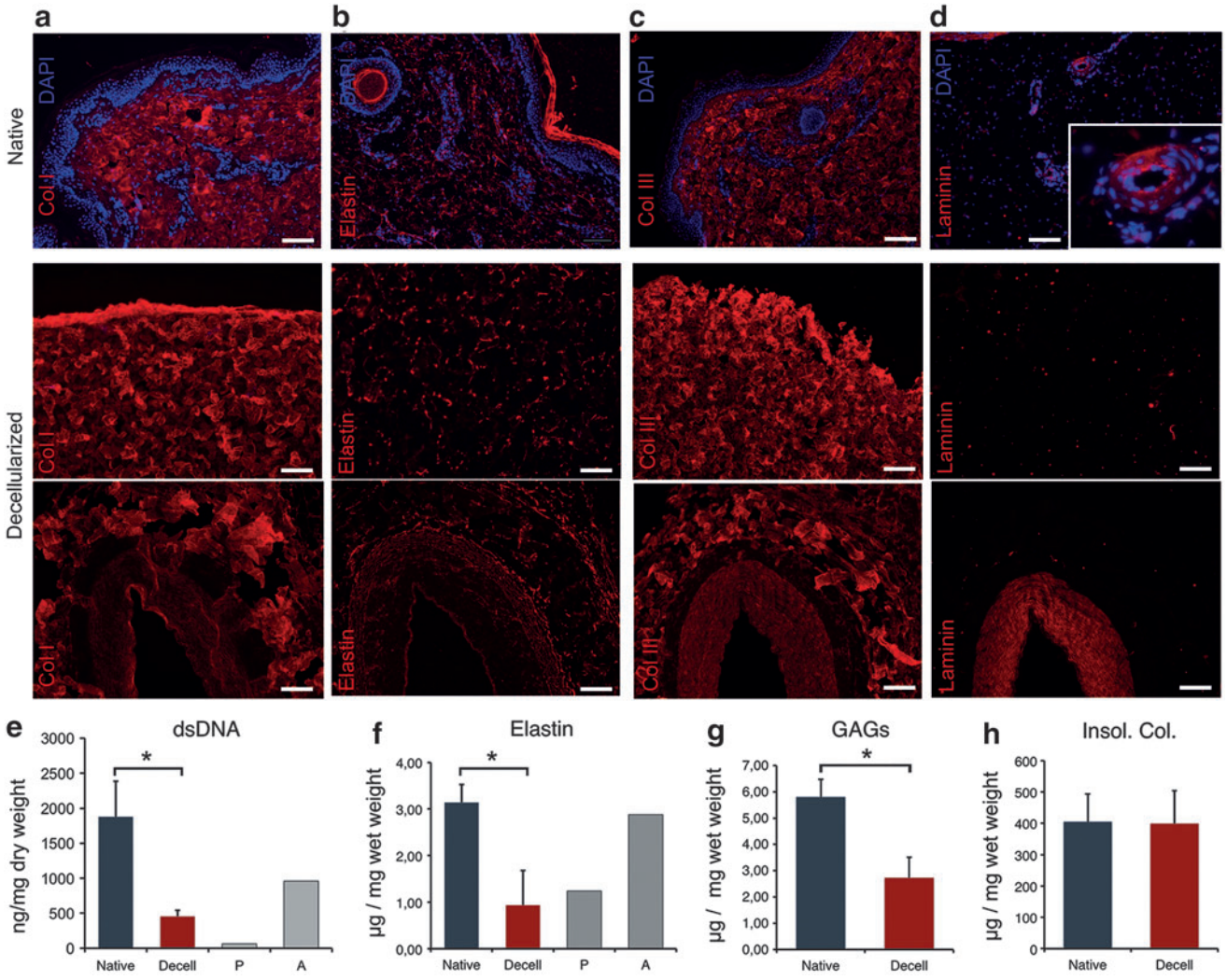

FIG. 3. ECM preservation and biochemical analysis. Immunofluorescent staining of native (*top*) and decellularized (*bottom*) tissue for collagen I **(a)**, elastin **(b)**, collagen III **(c)**, and laminin **(d)**. Biochemical quantification of DNA **(e)**, elastin **(f)**, glycosaminoglycan **(g)**, and insoluble collagen **(h)** content of native and decellularized tissue and Alloderm and Permacol for comparison of DNA and elastin content. $n > 3$ for native and decellularized samples, values are mean ± standard deviation, *asterisk* indicating $p < 0.05$. Scale bars 100 µm **(a–d)**.

For the *in vitro* test, SFSs were trimmed to preserve the superficial papillary dermis for culture (1000 µm). Seven days after cell seeding, we switched to modified complete EpiLife medium and elevated the regenerated dermal graft to an air/liquid interface to induce stratification. After 9 days at the air/liquid interface, formation of an epidermis-like structure was observed by histological analysis (Fig. 4e–g).

We found that keratinocytes formed a bioengineered epidermis-like structure formed on the acellular scaffold and ultimately established a stratified barrier (Fig. 4e). This newly formed tissue stained positive for pan-cytokeratin similar to native epidermis (Fig. 4f) and was impermeable to biotin penetration (Fig. 4g).

In vivo *immunological response and host incorporation*

To test for the immunological response of a host organism to our SFS, we performed an implantation study into xenogeneic rats. Five groups were used: native porcine skin, decellularized SFS, Alloderm, Permacol, and sham surgery. After 14 days, we observed the least degree of tissue integration for Permacol (Fig. 5d), with only marginal cellular infiltration and no detectable neovascular structures within the implanted matrix. Alloderm and native porcine skin both showed moderate tissue integration (Fig. 5a, b).

The native skin implants attracted significant immune cells, particularly on the epidermal side. Deformation of the implants, similar to wound contracture, was also noted. Alloderm showed mild cellular infiltration, similar to the native porcine skin, but without the immune response. Neovascular structures were not detectable.

SFS, in contrast, showed an extensive cellular infiltrate and an ill-defined, irregular border between the matrix and surrounding soft tissue (Fig. 5c). Quantification of the infiltrated area at the center of the implants showed almost 100% infiltration for the decellularized graft, followed by native skin implant (50% ± 19%), Alloderm (48% ± 3.9%), and Permacol (10%) (Fig. 5e). The majority of infiltrating cells for all groups were immune cells (CD68+CD3 combined, 78% for Sham and Permacol; 89%

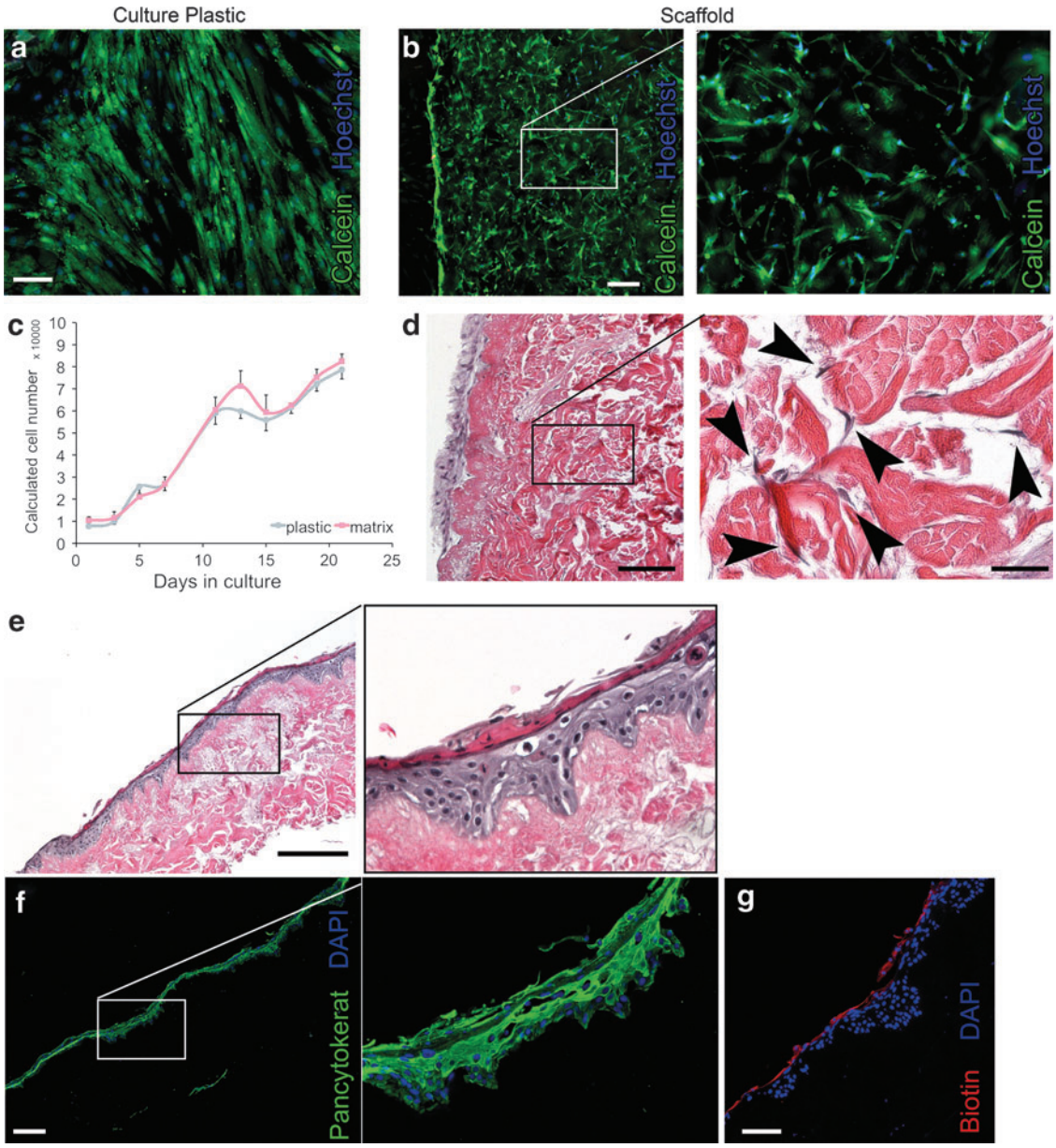

FIG. 4. Biocompatibility and regenerative potential *in vitro*. Calcein staining of hMSCs grown on culture plastic **(a)** or decellularized dermis **(b)**. **(c)** Growth curve of hMSCs cultured in six-well plates or decellularized dermis calculated from resazurin reduction assay according to the standard curve. Assay was performed every other day. $n=3$ per group. **(d)** H&E staining of hMSCs migrating into the decellularized dermis (*black arrowheads*). **(e)** H&E staining of re-epidermialized decellularized dermis. **(f)** Immunofluorescence staining for pan-cytokeratin in re-epidermialized dermis. **(g)** Biotin assay for analysis of barrier function of regenerated epidermis. Scale bars 100 μm **(a, d** blowup, **g)**; 200 μm **(b, f)**; 250 μm **(e)**; 500 μm **(d)**.

for decellularized SFS; 95% for Alloderm; and 100% for native implants; Fig. 5g, h). The number of cells per high-power field was comparable in native, decellularized, and Alloderm, while it was significantly lower for sham and Permacol (Fig. 5f).

Furthermore, we observed neovascularization with formation of capillaries within our SFS (Fig. 5c, high-power field, right) while retaining its tissue morphology (Fig. 5c, dermis = D and subcutis = S.C.). Quantification for pan-macrophage surface marker (CD68) in the infiltrating cell population showed the highest percentage of macrophages in the native skin implants (69% ± 0.9%) followed by Permacol (55.5% ± 7.6%) and Alloderm (53.9 ± 10.1), compared to 40.2% ± 10.8% for the decellularized skin scaffold and 33.9% ± 3.3% for the sham group (Fig. 5g). Quantification of pan-lymphocyte cell marker (CD3) showed no significant difference between the sham, native, decellularized, and Alloderm implants. Permacol attracted significantly lower CD3-positive cells compared to the sham group.

Analysis of whole blood samples from implanted rats was also performed. No statistically significant difference in white blood cell count, lymphocyte count, or monocyte (MONO) counts (Fig. 5i–k) was noted between the groups.

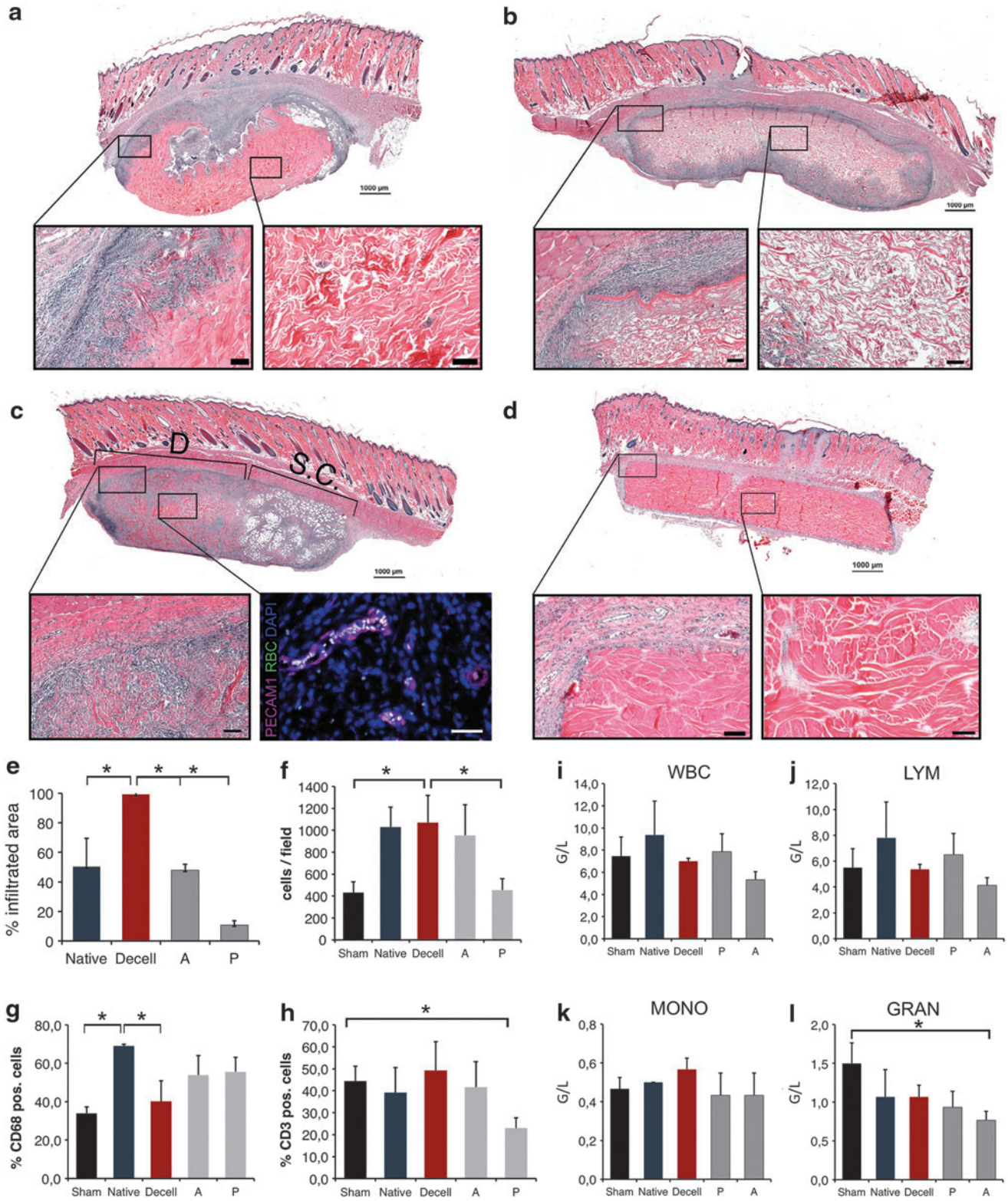

FIG. 5. Immunological response *in vivo*. H&E-stained cross sections 14 days after subcutaneous implantation with adjacent skin of the recipient animal for native implants **(a)**, Alloderm **(b)**, decellularized implants **(c)**, and Permacol **(d)**. **(c)** High-power field, *right*: immunofluorescent stain for endothelial cells (PECAM1) and RBC. **(e)** Quantification of cell infiltration as percentage of infiltrated cross-sectional area. **(f)** Quantification of cells per field at the implant border. Quantification of CD68-positive **(g)** and CD3-positive **(h)** cells as percentage of total cells per field. Quantification of whole blood analysis for WBC **(i)**, LYM (**j**), MONO **(k)**, and GRAN **(l)**. $n > 3$, values are mean ± standard deviation, *asterisk* indicating $p < 0.05$. Scale bars: 50 µm **(c,** IF high-power field, *right*); 100 µm **(a–d**, high-power fields); 1000 µm **(a–d)**. GRAN, granulocytes; IF, immunofluorescence; LYM, lymphocytes; MONO, monocytes; RBC, red blood cells; WBC, white blood cells.

Regenerative potential in vivo

The observed high degree of biocompatibility *in vitro* and *in vivo*, and especially the successful structure formation of keratinocytes *in vitro*, inspired us to attempt an *in vivo* test for the regenerative potential of our decellularized skin graft. We therefore implanted 6 mm biopsies from our SFS into a full-thickness skin defect in rats (Fig. 6a). The animals quickly recovered and showed no sign of pain or distress. Wound dressing was removed after 4 days, at which point the implant was scabbed over (Fig. 6b). Sutures were removed after 14 days. The crust fell off after ~20 days and revealed a pink neo-skin (Fig. 6c). In histological examination, we observed a fully infiltrated graft (Fig. 6d, e) and neovascularization extended into the center of the graft (Fig. 6e). The surface of the graft was completely covered by regenerated epidermis, which was microscopically similar to native rat epidermis (Fig. 6d, f) The neo-skin expressed

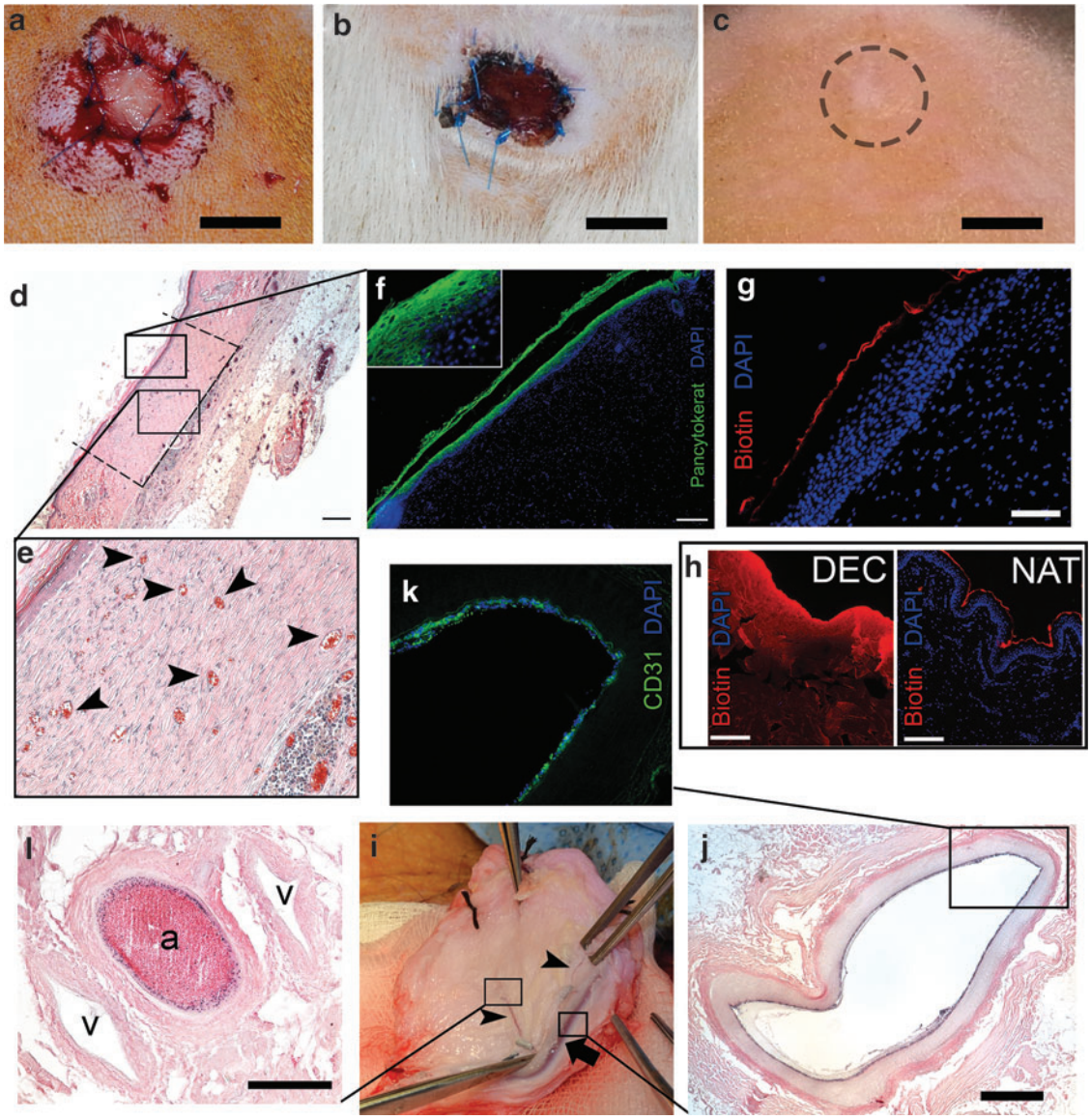

FIG. 6. Regenerative potential *in vivo* and experimental transplantation. **(a–c)** Photographs of full-thickness skin defect model covered with acellular porcine skin scaffold. **(a)** Immediately postoperative. **(b)** Wound at day 14, before suture removal. **(c)** Fully integrated skin scaffold on day 20. **(d)** Cross section of the skin with adjacent subcutaneous tissue, the whole graft (*dashed lines*) was re-epithelialized and extensively neovascularized. **(e)** *Black arrowheads* indicating neovascular structures within the implanted skin scaffold filled with RBCs. **(f)** The regenerated epithelium stained positive for pan-cytokeratin. **(g)** Biotin assay showing intact barrier function of the regenerated epidermis. **(h)** Biotin permeation in decellularized skin scaffold (*left*) and intact barrier function in native skin (*right*) as controls. **(i)** Re-endothelialized skin flap after reperfusion through the recipient's blood supply. *Black arrow* indicating vascular pedicle, *black arrowheads* indicating perfused branches. **(j)** H&E-stained cross section of the vascular pedicle after perfusion showing CD31-positive neoendothelium **(k)**. **(l)** H&E staining showing RBCs intraluminal of the arterial branch (a), while venous vessels (v) show no neoepithelium. Scale bars 100 μm **(g, h)**; 200 μm **(f, l)**; 250 μm **(d)**; 500 μm **(a, b, c, j)**.

pan-cytokeratin as seen in native skin (Fig. 6f) and showed barrier function against the environment, which was tested using the biotin assay described for the *in vitro* experiment (Fig. 6g).

Re-endothelialization and experimental transplantation

Immediate reperfusion after transplantation is crucial for the survival of transplanted tissue. We therefore re-endothelialized SFSs with HUVECs through the arterial pedicle. Within 5 days of culture, we noticed a decrease in vascular resistance (data not shown) and interpreted it as a sign of improving vascular barrier function.[27] Subsequently, we attempt an experimental transplantation in orthotopic position. On unclamping, we observed rapid inflow into the arterial pedicle, however, we were not able to observe venous outflow. Histological analysis showed endothelial coverage of the arterial pedicle and branches down to a size of 300 μm in diameter.

Discussion

Wounds, burns, and soft tissue loss are in many instances life-threatening injuries requiring intensive and highly specialized multidisciplinary care, frequent reinterventions, and often result in long recovery times and permanent disability. Despite several surgical treatment options and many commercially available dermal matrices, clinical outcomes are not optimal. One approach to the inherent challenges of matrix-based reconstruction is to utilize acellular matrices with a pre-existing, microvascular network. In recent years, tissue decellularization has been developed as a method for obtaining native ECM scaffolds.[5] Perfusion decellularization can generate native ECM scaffolds with intact vasculature and preserved tissue architecture from whole organs. Recellularization of these grafts has generated bioartificial organs such as the heart, lung, kidney, liver, and, more recently, a whole limb with rudimentary function.[6–8]

The results from the present study provide several steps forward toward the goal of creating a prevascularized, full-thickness skin flap of clinical scale. The technique of perfusion decellularization of fasciocutaneous flaps with an accessible vascular pedicle allows for the engineering of full-thickness, precellularized, skin flaps; and allows for complete penetration of the decellularization agent, which would not be possible with agitation alone. Perfusion decellularization allows for the optimal preservation of the natural ultrastructure of the ECM, and this enables optimal adhesion, proliferation, and differentiation of seeded cells.

In the herein reported experiments, we allowed a perfusion pressure of up to 200 mmHg and did not find any disruptions in the ECM of our decellularized skin by histologic examination. We found that perfusion decellularization removed all histologically visible cellular components from the tissue. The epidermis detached at the dermo–epidermal barrier, leaving behind intact papillary dermis for keratinocytes to attach. We confirmed decellularization by biochemical and histological analysis, which showed no remaining nuclei and decreased DNA content by ~77% to 455 ng/mg dry weight. This represents a medial residual DNA content between the two commercially available products Alloderm (950 ng DNA/mg tissue) and Permacol (63 ng DNA/mg tissue), evaluated using the same test. Residual DNA content can be further reduced by additional treatment with endonuclease.[11,28,29] We have previously applied endonuclease treatment to perfused tissue constructs to successfully reduce the dsDNA content below established thresholds for decellularized biomaterials (50 ng/mg).[28,30]

Previous studies have demonstrated that even fragmented dsDNA residing in decellularized biomaterials can elicit an enhanced proinflammatory response.[31–33] While recent studies suggest that disease transmission from decellularized xenogeneic ECM scaffolds is low, it is important to note that incomplete removal of cellular debris and other antigens can incite both innate and adaptive immune responses.[34–36] Advancement of this technology to the clinic would require further endonuclease treatment and characterization; however, it was not within the scope of this experimental study to meet the guidelines for residual DNA content in biomaterials.

In this work, we also performed an experiment on the immunological response of our decellularized SFS and compared it to xenogeneic skin grafts and two commercially available products. Fourteen days postimplantation, the SFS was fully infiltrated by cells, of which 90% represented immune cells, showed neovascularization and the highest degree of tissue integration into the recipient organism when compared to other matrix products. Quantification of the different types of infiltrating immune cells showed no significant difference between the decellularized implant and the sham group. Furthermore, implantation of the acellular skin grafts into full-thickness skin defects showed tissue integration and skin regeneration without cicatrization. Histologically, our decellularized skin flap showed local inflammation, cell infiltration, and neovascularization of the scaffold, similar to what can be observed in the inflammatory phase of wound healing.[37] However, more in-depth analysis of the cell dynamics and longer time points will be necessary to strengthen this conclusion.

The α-Gal epitope (Galalpha1-3Galbeta1-4GlcNAc-R) is the main antigen causing hyperacute rejection of porcine xenografts in primates.[38] In this study, however, we did not assess the residual α-Gal content of our SFS. Since α-Gal is mainly a cell membrane-bound glycoprotein, it is reduced by decellularization as shown in a recent study,[39] and can be further reduced by α-galactosidase if required.[38] Notably, acellular biomaterials derived from porcine tissues such as porcine small intestinal submucosa, which are recognized for retained α-Gal,[38] have been used clinically in millions of patients to date and have shown a constructive response rather than rejection.[40]

The mechanical properties of skin are extremely important for protection against injuries. To withstand mechanical stress, skin needs a high degree of reversible deformability—one of the major limitations of partial-thickness skin grafts and engineered skin replacements.[41] An ideal skin substitute should match the mechanical properties of surrounding host tissue.[42] The foundation of tissue biomechanical properties is the composition and ultrastructure of the ECM. Immunohistochemical and biochemical analysis indicate that our SFS has comparable molecular composition of the ECM protein collagen, elastin, and laminin as native skin. We performed biaxial testing and calculated the Young's modulus to test for the elastic properties of our SFS. We found that our decellularization protocol did not significantly affect elasticity compared to native skin. In this work, we showed that our full-thickness skin scaffold is biocompatible and has

an excellent regenerative potential for re-epithelialization, both *in vitro* and *in vivo*.

Immediate reperfusion of transplanted tissue is required to maintain viability; therefore, a vascular pedicle that can be anastomosed to the recipient's blood supply is critical. In this study, we were able to establish a protocol for the generation of a full-thickness SFS with a dominant vascular pedicle that we utilized for perfusion decellularization and seeding of endothelial cells. We noticed a decrease in vascular resistance during perfused tissue culture and interpreted this as improving barrier function of seeded endothelial cells.[27] Based on this observation, we attempted a transplantation experiment to test for perfusability *in vivo* into miniature swine; however, we did not observe venous outflow. Histology revealed re-endothelialization down to a vascular diameter of 300 μm. However, recellularization of microvasculature and capillary beds with much smaller vascular diameters (6 μm) was not observed. It is highly likely that incomplete re-endothelialization resulted in exposed collagen, which would have come into contact with circulating platelets that bind via collagen-specific glycoprotein Ia and IIa surface receptors to drive the coagulation cascade.

While the use of human endothelial cells with inherent human leukocyte antigens can cause an MHC mismatch that elicits skin graft rejection,[43] the short 1-h implantation time frame of our study makes this outcome unlikely. The miniature swine had not been previously exposed to human cells, and grafts were blood free before implantation, thereby reducing the chance for hyperacute rejection. Cell incompatibility due to MHC mismatch typically presents at longer survival durations as acute rejection. Reestablishment of functional endothelialized vascular channels throughout the entire scaffold is still a major hurdle and will ultimately require more sophisticated culturing protocols.[27] HUVECs are limited as an experimental cell source because they are allogeneic and relatively unspecific for generic use multiple tissue types. Recent work suggests that it is possible to generate tissue-specific endothelial cells from pluripotent sources,[44] theoretically making it possible to create patient-specific endothelial cell types for regenerated tissues of interest. Furthermore, a recent publication has shown great potential in the adipose stromal vascular fraction-derived endothelial cell population in generating a highly efficient capillary plexus in skin substitutes.[45]

In addition to endothelial cell types, more sophisticated culturing protocols will need to incorporate recellularization from both arterial and venous conduits.[27] Gradient perfusion pressures can also be incorporated, with low initial pressures to allow cell attachment and higher culturing pressures to allow cell migration and maturity within the matrix. A functional vascular network is a necessary prerequisite for the successful transplantation of a full-thickness SFS.

Conclusion

In the present study, we have developed a protocol for the generation of a full-thickness SFS of clinically relevant size, comprising a vascular pedicle, which can be utilized for perfusion decellularization and anastomosis to the recipient's vascular system after a precellularization process. We then analyzed our scaffold material extensively. First, we showed a high degree of biocompatibility and ability to support human keratinocyte engraftment and formation of epidermal-like tissue with intact barrier function. Second, we observed an immunological response indicative of biomaterial integration of our scaffold in an immunocompetent xenogeneic animal model. Third, we could achieve good regenerative potential of our scaffold *in vivo*, by preserving the biomechanical and biochemical properties of skin. Finally, we re-endothelialized a full-thickness SFS and attempted experimental transplantation in orthotopic position. However, in this last experiment, we were not able to establish full vascular perfusability. Future studies need to focus on the regeneration of the capillary network to allow for long-term transplantation experiments.

Acknowledgments

This work was supported by grants from the US National Institutes of Health (NIH) Director's New Innovator Award DP2 OD008749-01 and the Plastic Surgery Foundation/ Musculoskeletal Tissue Foundation (PSF/MTF) Dermal Tissue Grant.

Disclosure Statement

Dr. Goverman is a consultant for MIMEDX and has received consultation fees for his services. He also received a PSF/MTF award for the research presented here. He has no other competing financial interests. Dr. Ott is founder and stockholder of IVIVA Medical Inc, and this relationship did not affect the present study. Dr. Ott also receives grant support from United Therapeutics for unrelated projects in regenerative medicine. He has no other competing financial interests. For Drs. Jank, Guyette, Charest, Randolph, Gaudette, Gershlak, Purschke, Javorsky, Nazarian, Leonard, Cetrulo, and Austen, no competing financial interests exist.

References

1. Sen, C.K., *et al.* Human skin wounds: a major and snowballing threat to public health and the economy. Wound Repair Regen **17,** 763, 2009.
2. Ibrahim, A.E., Skoracki, R., Goverman, J., Sarhane, K.A., Parham, C.S., Abu-Sittah, G., Kaddoura, I., and Atiyeh, B.S. Microsurgery in the burn population—a review of the literature. Ann Burns Fire Disasters **28,** 39, 2015.
3. Philandrianos, C., *et al.* Comparison of five dermal substitutes in full-thickness skin wound healing in a porcine model. Burns **38,** 820, 2012.
4. Pham, C., Greenwood, J., Cleland, H., Woodruff, P., and Maddern, G. Bioengineered skin substitutes for the management of burns: a systematic review. Burns **33,** 946, 2007.
5. Jank, B.J., *et al.* Engineered composite tissue as a bioartificial limb graft. Biomaterials **61,** 246, 2015.
6. Ott, H.C., *et al.* Regeneration and orthotopic transplantation of a bioartificial lung. Nat Med **16,** 927, 2010.
7. Ott, H.C., *et al.* Perfusion-decellularized matrix: using nature's platform to engineer a bioartificial heart. Nat Med **14,** 213, 2008.
8. Song, J.J., *et al.* Regeneration and experimental orthotopic transplantation of a bioengineered kidney. Nat Med **19,** 646, 2013.
9. Petersen, T.H., *et al.* Tissue-engineered lungs for in vivo implantation. Science **329,** 538, 2010.

10. Uygun, B.E., *et al.* Organ reengineering through development of a transplantable recellularized liver graft using decellularized liver matrix. Nat Med **16,** 814, 2010.
11. Mertsching, H., *et al.* Generation and transplantation of an autologous vascularized bioartificial human tissue. Transplantation **88,** 203, 2009.
12. Raposio, E., Caruana, G., Bonomini, S., and Libondi, G. A novel and effective strategy for the isolation of adipose-derived stem cells: minimally manipulated adipose-derived stem cells for more rapid and safe stem cell therapy. Plast Reconstr Surg **133,** 1406, 2014.
13. Orazizadeh, M., Hashemitabar, M., Bahramzadeh, S., Dehbashi F.N., and Saremy, S. Comparison of the enzymatic and explant methods for the culture of keratinocytes isolated from human foreskin. Biomed Rep **3,** 304, 2015.
14. Chang, E.I., *et al.* Tissue engineering using autologous microcirculatory beds as vascularized bioscaffolds. FASEB J **23,** 906, 2009.
15. Henderson, P.W., *et al.* Development of an acellular bioengineered matrix with a dominant vascular pedicle. J Surg Res **164,** 1, 2010.
16. Qu, J., Van Hogezand, R.M., Hogezand, C., Zhao, B., Kuo, J., and Carlsen, B.T. Decellularization of a fasciocutaneous flap for use as a perfusable scaffold. Ann Plast Surg **75,** 112, 2015.
17. Guyette, J.P., *et al.* Perfusion decellularization of whole organs. Nat Protoc **9,** 1451, 2014.
18. Lunney, J.K., and Sachs, D.H. Transplantation in miniature swine. V. Characterization of Ia antigens. J Immunol **122,** 623, 1979.
19. Horner, B.M., *et al.* Induction of tolerance to an allogeneic skin flap transplant in a preclinical large animal model. Transplant Proc **41,** 539, 2009.
20. Carpenter, A.E., *et al.* CellProfiler: image analysis software for identifying and quantifying cell phenotypes. Genome Biol **7,** R100, 2006.
21. Jones, T.R., *et al.* Scoring diverse cellular morphologies in image-based screens with iterative feedback and machine learning. Proc Natl Acad Sci U S A **106,** 1826, 2009.
22. Freedman, B.R., *et al.* The (dys)functional extracellular matrix. Biochim Biophys Acta **1853(11 Pt B),** 3153, 2015.
23. Debels, H., Hamdi, M., Abberton, K., and Morrison, W. Dermal matrices and bioengineered skin substitutes: a critical review of current options. Plast Reconstruct Surg Global Open **3,** e284, 2015.
24. MacNeil, S. Progress and opportunities for tissue-engineered skin. Nature **445,** 874, 2007.
25. Hutcheon, A.E., Sippel, K.C., and Zieske, J.D. Examination of the restoration of epithelial barrier function following superficial keratectomy. Exp Eye Res **84,** 32, 2007.
26. Shimazaki, J., Higa, K., Kato, N., and Satake, Y. Barrier function of cultivated limbal and oral mucosal epithelial cell sheets. Invest Ophthalmol Vis Sci **50,** 5672, 2009.
27. Ren, X., *et al.* Engineering pulmonary vasculature in decellularized rat and human lungs. Nat Biotechnol **33,** 1097, 2015.
28. Guyette, J.P., *et al.* Bioengineering human myocardium on native extracellular matrix. Circ Res **118,** 56, 2016.
29. Moore, M.A., *et al.* Decellularization of human dermis using non-denaturing anionic detergent and endonuclease: a review. Cell Tissue Bank **16,** 249, 2015.
30. Crapo, P.M., Gilbert, T.W., and Badylak, S.F. An overview of tissue and whole organ decellularization processes. Biomaterials **32,** 3233, 2011.
31. Nagata, S., Hanayama, R., and Kawane, K. Autoimmunity and the clearance of dead cells. Cell **140,** 619, 2010.
32. Zheng, M.H., *et al.* Porcine small intestine submucosa (SIS) is not an acellular collagenous matrix and contains porcine DNA: possible implications in human implantation. J Biomed Mater Res B Appl Biomater **73,** 61, 2005.
33. Keane, T.J., Londono, R., Turner, N.J., and Badylak, S.F. Consequences of ineffective decellularization of biologic scaffolds on the host response. Biomaterials **33,** 1771, 2012.
34. Garkavenko, O., *et al.* Monitoring for presence of potentially xenotic viruses in recipients of pig islet xenotransplantation. J Clin Microbiol **42,** 5353, 2004.
35. Garkavenko, O., *et al.* Absence of transmission of potentially xenotic viruses in a prospective pig to primate islet xenotransplantation study. J Med Virol **80,** 2046, 2008.
36. Keane, T.J., and Badylak, S.F. The host response to allogeneic and xenogeneic biological scaffold materials. J Tissue Eng Regen Med **9,** 504, 2015.
37. Agaiby, A.D., and Dyson, M. Immuno-inflammatory cell dynamics during cutaneous wound healing. J Anat **195 (Pt 4),** 531, 1999.
38. McPherson, T.B., Liang, H., Record, R.D., and Badylak, S.F. Galalpha (1,3) Gal epitope in porcine small intestinal submucosa. Tissue Eng **6,** 233, 2000.
39. Jones, G., *et al.* Decellularization and characterization of porcine superflexor tendon: a potential anterior cruciate ligament replacement. Tissue Eng Part A **23,** 124, 2017.
40. Ansaloni, L., *et al.* Immune response to small intestinal submucosa (surgisis) implant in humans: preliminary observations. J Invest Surg **20,** 237, 2007.
41. Pawlaczyk, M., Lelonkiewicz, M., and Wieczorowski, M. Age-dependent biomechanical properties of the skin. Postepy Dermatol Alergol **30,** 302, 2013.
42. Bader, D.L., and Bowker, P. Mechanical characteristics of skin and underlying tissues in vivo. Biomaterials **4,** 305, 1983.
43. Shanmugarajah, K., *et al.* The effect of MHC antigen matching between donors and recipients on skin tolerance of vascularized composite allografts. Am J Transplant [Epub ahead of print]; DOI: 10.1111/ajt.14189.
44. Lippmann, E.S., *et al.* Derivation of blood-brain barrier endothelial cells from human pluripotent stem cells. Nat Biotechnol **30,** 783, 2012.
45. Klar, A.S., *et al.* Tissue-engineered dermo-epidermal skin grafts prevascularized with adipose-derived cells. Biomaterials **35,** 5065, 2014.

Address correspondence to:
Harald C. Ott, MD
Massachusetts General Hospital
Ott Lab for Organ Engineering
Richard B. Simches Research Center
MCPZN4700
185 Cambridge Street
Boston, MA 02116

E-mail: hott@partners.org

Received: November 8, 2016
Accepted: February 14, 2017
Online Publication Date: June 19, 2017